Article

Improving the Effectiveness of Interfacial Trapping in Removing Single-Walled Carbon Nanotube Bundles

Randy K. Wang, Hyun-Ok Park, Wei-Chiang Chen, Carlos Silvera-Batista, Ryan D. Reeves, Jason E. Butler, and Kirk J. Ziegler

J. Am. Chem. Soc., **2008**, 130 (44), 14721-14728 • DOI: 10.1021/ja804982b • Publication Date (Web): 11 October 2008

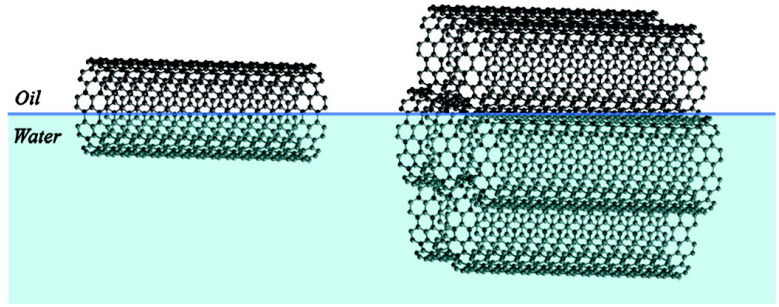

More About This Article

Additional resources and features associated with this article are available within the HTML version:

- Supporting Information
- Links to the 1 articles that cite this article, as of the time of this article download
- Access to high resolution figures
- Links to articles and content related to this article
- Copyright permission to reproduce figures and/or text from this article

View the Full Text HTML

J|A|C|S
ARTICLES

Published on Web 10/11/2008

Improving the Effectiveness of Interfacial Trapping in Removing Single-Walled Carbon Nanotube Bundles

Randy K. Wang,[†] Hyun-Ok Park,[†] Wei-Chiang Chen,[†] Carlos Silvera-Batista,[†] Ryan D. Reeves,[†] Jason E. Butler,[†] and Kirk J. Ziegler*[,†,‡]

Department of Chemical Engineering, and Center for Surface Science and Engineering, University of Florida, Gainesville, Florida 32611

Received June 29, 2008; E-mail: kziegler@che.ufl.edu

Abstract: Single-walled carbon nanotube (SWNT) bundles are selectively removed from an aqueous dispersion containing individually suspended carbon nanotubes coated with gum Arabic via interfacial trapping. The suspensions are characterized with absorbance, fluorescence, and Raman spectroscopy as well as atomic force microscopy (AFM) and rheology. The resulting aqueous suspensions have better dispersion quality after interfacial trapping and can be further improved by altering the processing conditions. A two-step extraction process offers a simple and fast approach to preparing high-quality dispersions of individual SWNTs comparable to ultracentrifugation. Partitioning of SWNTs to the liquid−liquid interface is described by free energy changes. SWNT bundles prefer to reside at the interface over individually suspended SWNTs because of greater free energy changes.

Introduction

Single-walled carbon nanotubes (SWNTs) pack into bundles because of the strong van der Waals attractive forces.[1,2] High-energy ultrasonication is often used to overcome these forces to obtain individual SWNTs in solution. However, many common solvents have insufficient solvation forces to suspend SWNTs, yielding low degrees of solubility.[3] These suspensions consist of many small bundles and relatively few individual SWNTs. The difficulties associated with obtaining individually dispersed SWNTs limits nanotube applications,[1,4,5] leading researchers to develop a multitude of functionalization schemes to achieve nanotube suspensions.[5−8]

Noncovalent functionalization routes are preferred in many applications to preserve the properties of SWNTs. However, researchers have noted that these approaches yield a solution containing individual nanotubes as well as nanotube bundles.[9] The bundling of nanotubes diminishes the mechanical properties in nanocomposites since the SWNTs slip past one another under stress.[10] Bundled nanotubes also perturb the electronic structure of semiconducting SWNTs, quenching their intrinsic fluorescence.[9,11,12] The conventional method to disperse individual nanotubes in aqueous solutions is by high-shear homogenization in various surfactant solutions[13,14] followed by ultrasonication and ultracentrifugation.[11] However, ultracentrifugation is a time-consuming approach to the removal of SWNT bundles. Therefore, alternative routes to remove bundles from SWNT suspensions are needed for economic, large-scale dispersion.

Recently, we described a simple alternative to ultracentrifugation using liquid−liquid interfaces to remove nanotube bundles from the aqueous SWNT suspension.[15] This technique has already been combined with density gradient ultracentrifugation[16] to significantly improve field-effect transistor performance.[17] The adsorption of colloidal particles at interfaces was first characterized by Pickering in 1907.[18] These systems have been used to self-assemble particles at the interface,[19,20] to

[†] Department of Chemical Engineering.
[‡] Center for Surface Science and Engineering.

(1) Shvartzman-Cohen, R.; Nativ-Roth, E.; Baskaran, E.; Levi-Kalisman, Y.; Szleifer, I.; Yerushalmi-Rozen, R. *J. Am. Chem. Soc.* **2004**, *126*, 14850.
(2) Girifalco, L. A.; Hodak, M.; Lee, R. S. *Phys. Rev. B* **2000**, *62*, 13104.
(3) Bahr, J. L.; Mickelson, E. T.; Bronikowski, M. J.; Smalley, R. E.; Tour, J. M. *Chem. Commun.* **2001**, 193.
(4) Rueckes, T.; Kim, K.; Joselevich, E.; Tseng, G. Y.; Cheung, C.-L.; Lieber, C. M. *Science* **2000**, *289*, 94.
(5) Banerjee, S.; Hemraj-Benny, T.; Wong, S. S. *Adv. Mater.* **2005**, *17*, 17.
(6) Bahr, J. L.; Tour, J. M. *J. Mater. Chem.* **2002**, *12*, 1952.
(7) Hirsch, A. *Angew. Chem., Int. Ed.* **2002**, *41*, 1853.
(8) Khabashesku, V. N.; Billups, W. E.; Margrave, J. L. *Acc. Chem. Res.* **2002**, *35*, 1087.
(9) Bachilo, S. M.; Strano, M. S.; Kittrell, C.; Hauge, R. H.; Smalley, R. E.; Weisman, R. B. *Science* **2002**, *298*, 2361.
(10) Ajayan, P. M.; Tour, J. M. *Nature* **2007**, *447*, 1066.
(11) O'Connell, M. J.; Bachilo, S. M.; Huffman, C. B.; Moore, V. C.; Strano, M. S.; Haroz, E. H.; Rialon, K. L.; Boul, P. J.; Noon, W. H.; Kittrell, C.; Ma, J.; Hauge, R. H.; Weisman, R. B.; Smalley, R. E. *Science* **2002**, *297*, 593.
(12) Jones, M.; Engtrakul, C.; Metzger, W. K.; Ellingson, R. J.; Nozik, A. J.; Heben, M. J.; Rumbles, G. *Phys. Rev. B* **2005**, *71*, 115426.
(13) Bandyopadhyaya, R.; Nativ-Roth, E.; Regev, O.; Yerushalmi-Rozen, R. *Nano Lett.* **2002**, *2*, 25.
(14) Moore, V. C.; Strano, M. S.; Haroz, E. H.; Hauge, R. H.; Smalley, R. E. *Nano Lett.* **2003**, *3*, 1379.
(15) Wang, R. K.; Reeves, R. D.; Ziegler, K. J. *J. Am. Chem. Soc.* **2007**, *129*, 15124.
(16) Arnold, M. S.; Green, A. A.; Hulvat, J. F.; Stupp, S. I.; Hersam, M. C. *Nat. Nanotechnol.* **2006**, *1*, 60.
(17) Lee, C. W.; Weng, C.-H.; Wei, L.; Chen, Y.; B, C.-P. M.; Tsai, C.-h.; Leou, K.-c.; Poa, C. H. P.; Glerup, M.; Wang, J.; Li, L.-J. *J. Phys. Chem. C* **2008**, *112*, 12089.
(18) Pickering, S. U. *J. Chem. Soc, Trans.* **1907**, *91*, 2001.
(19) Lin, Y.; Skaff, H.; Emrick, T.; Dinsmore, A. D.; Russell, T. P. *Science* **2003**, *299*, 226.
(20) He, J.; Zhang, Q.; Gupta, S.; Emrick, T.; Russell, T. R.; Thiyagarajan, P. *Small* **2007**, *3*, 1214.

separate particles, such as ampicillin and phenylglycine crystal mixtures in water/alkanol systems,[21,22] and to prepare unique porous structures.[23] Pickering systems have also demonstrated the large-scale separation of bioparticles, achieving efficiencies greater than centrifugation.[24] Wang, Hobbie and co-workers[25,26] were the first to show SWNT-based stabilization of emulsions. Bare nanotubes were used as amphiphobic surfactants that stabilized toluene/water emulsions for months.[25] Later, DNA-wrapped SWNTs were shown to stabilize emulsions for the synthesis of colloidal particles.[26] Stabilized emulsions were also seen in length-based separations of functionalized SWNTs.[27] More recently, researchers have begun to use SWNT-based Pickering emulsions for other applications. Asuri et al.[28] demonstrated that interfacial SWNTs decreased transport limits and improved catalytic activity of two-phase reactions leading to increased bioreactivity. Others used polymerization reactions[29,30] or nanotube interactions[31] to prepare nanotube capsules for supports, controlled release capsules,[31] and lubricating additives.[23]

In this paper, further details are provided on the method and mechanism of the interfacial trapping process for removing nanotube bundles from aqueous suspensions. Near-infrared (NIR) fluorescence, vis−NIR absorbance, and Raman spectroscopy as well as atomic force microscopy (AFM) and rheology are used to characterize the SWNT suspensions. New approaches to improve dispersion quality are also discussed. The suspensions prepared by interfacial trapping have comparable dispersion quality to those prepared by ultracentrifugation.

Experimental Section

Dispersion. Nanotube suspensions were prepared with a given initial mass (typically between 6 and 20 mg) of raw SWNTs (Rice HPR 145.1) and mixed with 200 mL of an aqueous gum Arabic (Sigma-Aldrich) surfactant solution[13] (1 wt %) to form an initial concentration of 0.03−0.2 mg/mL. High-shear homogenization (IKA T-25 Ultra-Turrax) for 1 h and ultrasonication (Misonix S3000) for 10 min aided dispersion. Control samples were ultracentrifuged at speeds between 20 000 and 26 000 rpm (Beckman Coulter Optima L-80 K) for 4−5 h to remove nanotube bundles.

Interfacial Trapping. Toluene (Acros, 99%) was added to the aqueous SWNT suspension to form a two-phase system. The two-phase system was then shaken vigorously for 30 s to increase interfacial area. Phase separation occurs within 1−2 min; however, the solutions were allowed to settle for 30−60 min to ensure that steady state was achieved for spectroscopy. All experiments were conducted at an organic to aqueous SWNT suspension volume ratio of 0.1 unless otherwise indicated.

Characterization. The aqueous phase was carefully removed after interfacial trapping to prevent further emulsification. The aqueous phase was characterized by vis−NIR absorbance and NIR fluorescence spectra using an Applied NanoFluorescence Nanospectrolyzer (Houston, TX) with excitation from 662 and 784 nm diode lasers. A concentrated gum Arabic SWNT suspension was homogenized and ultrasonicated and then incrementally diluted with 1 wt % gum Arabic solution to determine the linear regions of the absorbance and fluorescence spectra (Figures S1 and S2 in the Supporting Information). Raman spectra were recorded using a Renishaw Invia Bio Raman with excitation from a 785 nm diode laser. SWNT suspensions were also spin-coated onto mica to collect AFM images on a Digital Instruments Dimension 3100. Diameter analysis was then performed using SIMAGIS software.[32] A minimum of 700 nanotubes were measured for statistically relevant results. The rheology of SWNT suspensions was examined using an ARES LS-1 strain-controlled rheometer (TA Instruments). A cone and plate fixture with a diameter of 50 mm and an angle of 0.04 rad was used to measure the steady shear viscosity at rates between 1 and 100 s^{-1}. As an additional step in preparing the interfacial trapped samples for rheological characterization, the gum Arabic solution was initially centrifuged at 26 000 rpm for 30 min before adding nanotubes. Solutions of gum Arabic, prior to centrifugation, showed variations in rheology, consistent with other reports.[33,34] The additional processing produced a stable solution of gum Arabic with a viscosity of 1.68 ± 0.05 cP as measured over the entire range of shear rates. For rheological characterization, SWNT suspensions were ultracentrifuged for 2 h to prepare similar final concentrations for analysis (determined using the extinction coefficient[35,36] and absorbance at 763 nm).

Results and Discussion

Selective Separation of Bundles. After mixing toluene with a homogenized and ultrasonicated aqueous suspension, the system forms a homogeneous gray solution of emulsions. An interphase of emulsions and a bulk aqueous phase forms within a minute as seen in the inset of Figure 1. Absorbance spectra of the bulk aqueous phase are shown in Figure 1a. The homogenized and ultrasonicated sample (control) has high absorbance due to the concentration of both individual (as evidenced by the interband transition peaks) and bundled SWNTs. The absorbance of the suspension has clearly decreased after interfacial trapping while the spectral features have blue-shifted and are better resolved. These changes indicate the removal of nanotubes from the aqueous phase and a higher fraction of individual SWNTs.[37] When the control suspension is ultracentrifuged, the absorbance of the aqueous phase is significantly lower demonstrating that ultracentrifugation removes a significant portion of the nanotubes (both bundled and individual) at the relatively low concentrations used here.

Fluorescence spectra of the aqueous phase are shown in Figure 1b. For comparison, the spectum after homogenization and ultrasonication is shown (control) as well as the spectrum using conventional ultracentrifugation rather than interfacial

(21) Jauregi, P.; Hoeben, M. A.; van der Lans, R. G. J. M.; Kwant, G.; van der Wielen, L. A. M. *Ind. Eng. Chem. Res.* **2001**, *40*, 5815.
(22) Jauregi, P.; Hoeben, M. A.; van der Lans, R. G. J. M.; Kwant, G.; van der Wielen, L. A. M. *Biotechnol. Bioeng.* **2002**, *78*, 355.
(23) Lu, H. F.; Fei, B.; Xin, J. H.; Wang, R. H.; Li, L.; Guan, W. C. *Carbon* **2007**, *45*, 936.
(24) Hoeben, M. A.; van der Lans, R. G. J. M.; van der Wielen, L. A. M.; Kwant, G. *AIChE J.* **2004**, *50*, 1156.
(25) Wang, H.; Hobbie, E. K. *Langmuir* **2003**, *19*, 3091.
(26) Hobbie, E. K.; Bauer, B. J.; Stephens, J.; Becker, M. L.; McGuiggan, P.; Hudson, S. D.; Wang, H. *Langmuir* **2005**, *21*, 10284.
(27) Ziegler, K. J.; Schmidt, D. J.; Rauwald, U.; Shah, K. N.; Flor, E. L.; Hauge, R. H.; Smalley, R. E. *Nano Lett.* **2005**, *5*, 2355.
(28) Asuri, P.; Karajanagi, S. S.; Dordick, J. S.; Kane, R. S. *J. Am. Chem. Soc.* **2006**, *128*, 1046.
(29) Menner, A.; Verdejo, R.; Shaffer, M.; Bismarck, A. *Langmuir* **2007**, *23*, 2398.
(30) Panhuis, M. i. h.; Paunov, V. N. *Chem. Commun.* **2005**, 1726.
(31) Yi, H.; Song, H.; Chen, X. *Langmuir* **2007**, *23*, 3199.
(32) Ziegler, K. J.; Rauwald, U.; Gu, Z.; Liang, F.; Billups, W. E.; Hauge, R. H.; Smalley, R. E. *J. Nanosci. Nanotechnol.* **2007**, *7*, 2917.
(33) Sanchez, C.; Renard, D.; Robert, P.; Schmitt, C.; Lefebvre, J. *Food Hydrocolloids* **2002**, *16*, 257.
(34) Yaseen, E. I.; Herald, T. J.; Aramouni, F. M.; Alavi, S. *Food Res. Int.* **2005**, *38*, 111.
(35) Parra-Vasquez, A. N. G.; Stepanek, I.; Davis, V. A.; Moore, V. C.; Haroz, E. H.; Shaver, J.; Hauge, R. H.; Smalley, R. E.; Pasquali, M. *Macromolecules* **2007**, *40*, 4043.
(36) Moore, V. C. Single walled carbon nanotubes: Suspension in aqueous/surfactant media and chirality controlled synthesis on surfaces. Ph.D. Dissertation, Rice University, Houston, TX, 2005.
(37) Tan, Y.; Resasco, D. E. *J. Phys. Chem. B* **2005**, *109*, 14454.

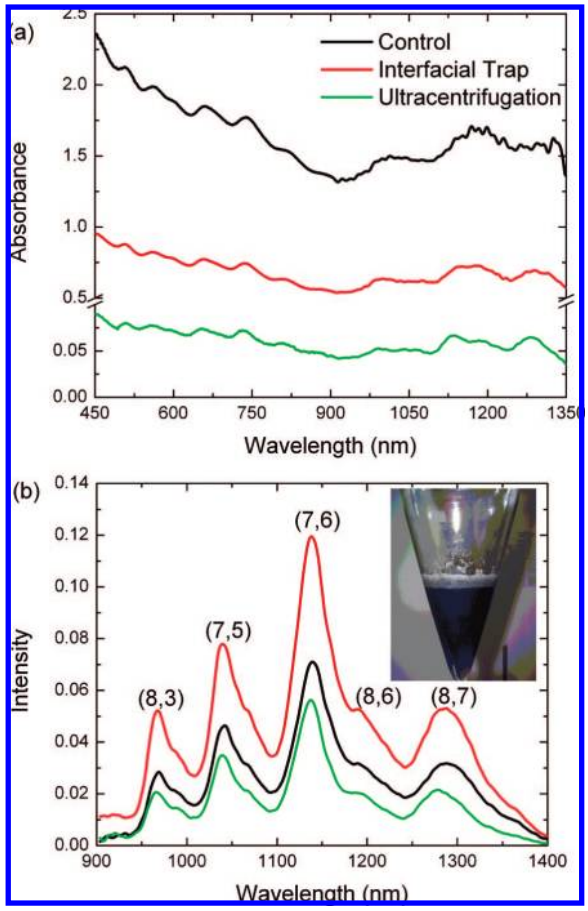

Figure 1. (a) Absorbance and (b) fluorescence (ex = 662 nm) spectra for the interfacial trapping process of gum Arabic-suspended SWNTs using an initial SWNT mass concentration of 0.03 mg/mL. The control spectra (black lines) are the SWNTs after homogenization and ultrasonication. The inset shows the interfacial trapping process in a separatory funnel. The control sample is then either subjected to ultracentrifugation (green lines) or interfacial traps (red lines). The fluorescence from specific (n, m) types are labeled.

trapping. The spectra show that ultracentrifugation results in a decrease in fluorescence intensity indicative of the removal of individual nanotubes. However, the fluorescence intensity after interfacial trapping increases when compared to the control sample. It is also important to note that the peak positions for both the interfacial trapped and ultracentrifuged suspensions are identical, indicating that the environment surrounding the nanotube has not changed after mixing with the solvent.

Fluorescence intensities are related to the concentration of individual nanotubes. Fluorescence spectra also provide a sensitive probe to the aggregation state of the aqueous phase.[11,38] Typically, higher intensity peaks in the spectra indicate better dispersion quality[38] since energy transfer can occur between adjacent nanotubes in bundles resulting in either intensity changes or complete quenching of the fluorescence.[9,12] This energy transfer mechanism can also occur between individual SWNTs. Recently, several groups[39−41] have observed that energy transfer between SWNTs results in fluorescence changes. The fluorescence intensity of individually suspended SWNTs may decay as the volume fraction increases as observed in solid composites.[42] Concentrated SWNT suspensions could also potentially reabsorb emitted photons thereby reducing the measured emission intensity. However, the dilute initial SWNT concentration (0.03 mg/mL) is in the linear region of both fluorescence and absorbance measurements (see Figures S1 and S2 in the Supporting Information). Therefore, the increase in fluorescence intensity observed in Figure 1b is likely due to reduced quenching after interfacial trapping. Removal of nanotubes from the solution, especially SWNT bundles that quench fluorescence, would allow more individual, semiconducting SWNTs to emit photons, resulting in increased fluorescence intensities.

SWNT suspensions with a much lower concentration were used during interfacial trapping (0.005 mg/mL) to test whether the enhancement of the fluorescence seen in Figure 1 was due to the removal of SWNT bundles. The lower initial concentration results in fewer collisions between nanotubes and, thus, fewer potential quenching events. At these concentrations, changes to the number of quenching bundles in the suspension should have a reduced effect on the spectra. Figure 2a shows that fluorescence at low concentrations has only a slight change after interfacial trapping, whereas the absorbance in Figure 2b has diminished significantly. Since the fluorescence remains relatively constant, the clear decrease in absorbance can only be attributed to the removal of bundles or other carbonaceous impurities from the aqueous phase, suggesting that selective bundle removal occurs.

Dispersion Quality. Quantifying the fraction of individually suspended SWNTs or bundles in an aqueous solution remains difficult.[38] Rheology,[35,38] fluorescence,[11,12,38] Raman,[38,43] absorbance,[37] and small-angle neutron scattering (SANS)[26,38,44,45] have already been successfully used to study the interactions of surfactant-coated SWNTs in aqueous solutions. Visual methods such as AFM are also used to obtain qualitative and quantitative information about the dispersion.[32,46] The group from NIST recommended that multiple techniques be used to quantify dispersion.[38] Several techniques that describe the dispersion quality of the aqueous suspension after interfacial trapping are discussed below. A higher initial SWNT concentration of 0.2 mg/mL was used to investigate the dispersion quality, and the results are summarized in Table 1.

Parts a and b of Figure 3 show AFM images of the homogenized and ultrasonicated SWNT suspension compared to the suspension after interfacial trapping. Corresponding histograms of nanotube diameters are shown in Figure 3c. As expected, the homogenized and ultrasonicated SWNT suspension has many bundled SWNTs and some individually suspended SWNTs (diameters less than ~3 nm), yielding a broad diameter distribution with an average of 12.8 nm. After interfacial trapping, the suspension has significantly fewer

(38) Fagan, J. A.; Landi, B. J.; Mandelbaum, I.; Simpson, J. R.; Bajpai, V.; Bauer, B. J.; Migler, K.; Hight Walker, A. R.; Raffaelle, R.; Hobbie, E. K. *J. Phys. Chem. B* **2006**, *110*, 23801.
(39) Qian, H.; Georgi, C.; Anderson, N.; Green, A. A.; Hersam, M. C.; Novotny, L.; Hartschuh, A. *Nano Lett.* **2008**, *8*, 1363.
(40) Tan, P. H.; Rozhin, A. G.; Hasan, T.; Hu, P.; Scardaci, V.; Milne, W. I.; Ferrari, A. C. *Phys. Rev. Lett.* **2007**, *99*, 137402+
(41) Torrens, O. N.; Milkie, D. E.; Zheng, M.; Kikkawa, J. M. *Nano Lett.* **2006**, *6*, 2864.
(42) Graff, R. A.; Swanson, J. P.; Barone, P. W.; Baik, S.; Heller, D. A.; Strano, M. S. *Adv. Mater.* **2005**, *17*, 980.
(43) O'Connell, M. J.; Sivaram, S.; Doorn, S. K. *Phys. Rev. B* **2004**, *69*, 235415.
(44) Zhou, W.; Islam, M. F.; Wang, H.; Ho, D. L.; Yodh, A. G.; Winey, K. I.; Fischer, J. E. *Chem. Phys. Lett.* **2004**, *384*, 185.
(45) Wang, H.; Zhou, W.; Ho, D. L.; Winey, K. I.; Fischer, J. E.; Glinka, C. J.; Hobbie, E. K. *Nano Lett.* **2004**, *4*, 1789.
(46) Islam, M. F.; Rojas, E.; Bergey, D. M.; Johnson, A. T.; Yodh, A. G. *Nano Lett.* **2003**, *3*, 269.

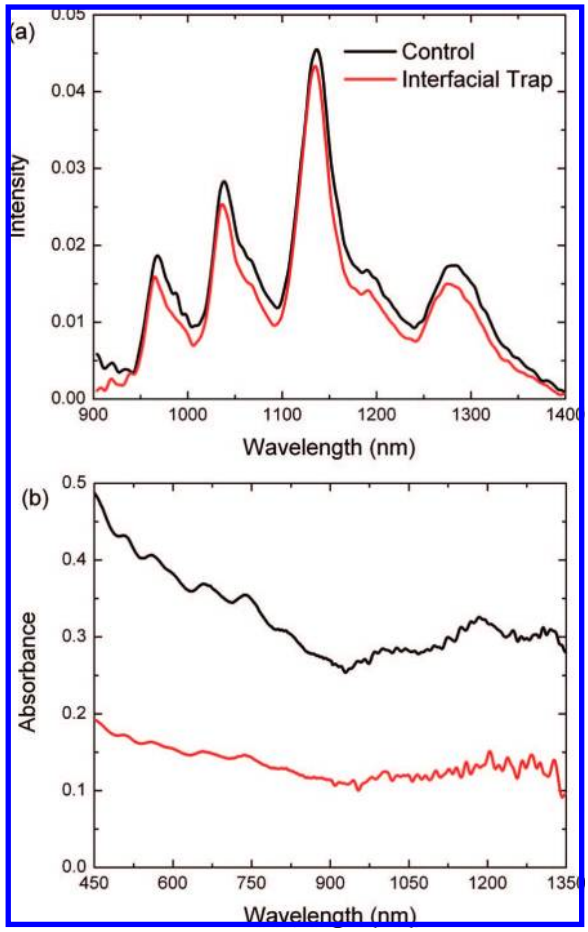

Figure 2. (a) Absorbance and (b) fluorescence (ex = 662 nm) spectra of SWNTs at a concentration of 0.005 mg/mL. The control spectra (black lines) are the SWNTs after homogenization and ultrasonication. The control sample is then subjected to interfacial traps.

bundled SWNTs and a sharper distribution in diameters with an average of 4.1 nm. A significant fraction of the population after interfacial trapping is individually dispersed SWNTs.

The relative intensity of the interband transition peaks in the absorbance spectra and their width are related to the dispersion quality.[11,37,38] Tan and Resasco[37] showed that the resonance ratio could be used to characterize the fraction of individual SWNTs in solution. This ratio is calculated by comparing the area for the resonant band with the nonresonant band (carbonaceous impurities and π-plasmon). The interfacial trapping method shows improved dispersion characteristics and improved fractions of individually suspended SWNTs.

Figure 4 is the Raman spectra of the SWNT radial breathing modes (RBMs). The peak at $\sim$270 cm^{-1} represents the shift of (10, 2) nanotubes due to bundling, providing a measure of the extent of nanotube aggregation.[47] The homogenized and ultrasonicated suspension has a very intense aggregation peak in comparison to the (11, 3) nanotubes at $\sim$234 cm^{-1}. As seen in Figure 4 and Table 1, the ratio of these peaks drops dramatically after interfacial trapping, indicating removal of bundled SWNTs.

Figure 5 compares the steady values of the shear viscosities for the three different SWNT suspensions. The viscosity of all systems nearly matches at the highest shear rate of 100 s^{-1}, demonstrating that the small difference in concentration across the three systems has a limited impact on the results. Differences in the rheology are apparent at lower shear rates. Except for the lowest shear rate, the control sample has a nearly constant viscosity as a function of shear rate. The ultracentrifugation and interfacial trapping methods produce samples that shear thin. The decrease in viscosity with increasing shear rate is more pronounced for the ultracentrifugation sample but agrees within measurement error with the result from the sample prepared using interfacial trapping. The favorable comparison implies that our method produces a suspension of nanotubes similar in flow characteristics, and hence dispersion quality, to the ultracentrifugation method.

The fluorescence intensity provides a measure of the concentration of individually suspended SWNTs but does not account for variations in total concentration (i.e., fraction of individual SWNTs). On the other hand, the absorbance provides an overall measure of the entire ensemble of individual and bundled SWNTs, providing a means of normalizing the fluorescence intensity. The ratio of fluorescence to absorbance (F/A), therefore, is another measure of dispersion quality. This ratio should be the most relevant measurement to many applications since it is related to the quantum yield of the nanotube suspension. Note that this ratio is not a quantitative measure of the fraction of individual SWNTs and it should only be used to compare dispersion characteristics between samples. In this study, the intensity from the (7, 6) nanotube is used and divided by the absorbance at the excitation wavelength (662 nm). The decrease in absorbance and increase in fluorescence cause the F/A ratio to improve after interfacial trapping as shown in Table 1.

Improving Separation Effectiveness. In summary, the SWNT suspension resulting from a single-step interfacial trapping process has improved dispersion quality in comparison to homogenized and ultrasonicated suspensions as shown in Table 1. SWNT dispersions prepared by ultracentrifugation have higher dispersion quality, but one of the benefits of the interfacial trapping method is that the process can be easily adjusted to change separation efficiency. Figure 6 shows the variation of fluorescence emission intensity of the most prominent (7, 6) nanotube type in the spectra as a function of the volume ratio of toluene to the aqueous SWNT suspension ($R = V_{toluene}/V_{aqueous}$). As seen in Figure 6a for an initial SWNT mass concentration of 0.03 mg/mL, higher fluorescence intensity is observed for $R \geq 1$. The higher conductivity of the solution when $R > 1$ suggests that water-in-oil (w/o) emulsions are formed, whereas oil-in-water (o/w) emulsions are seen for $R < 1$. It is also seen that the fluorescence intensity is always greater than the control for initial mass loadings of 0.03 mg/mL. Figure 6b shows the fluorescence intensity from an initial mass loading of 0.005 mg/mL of SWNTs. As can be seen in the figure, the emission intensity tends to be lower than the control for o/w emulsions, whereas w/o emulsions show relatively constant intensity. The same trends are seen for other emission peaks and other initial mass loadings (not shown).

Although the fluorescence intensity changes are relatively minor, the changes to the absorbance spectra in Figure 7a are significant. The absorbance spectra for all volume ratios has decreased significantly after interfacial trapping when compared to the control sample in Figure 1. The interband transition peaks are noticed for all aqueous solutions, indicating good dispersion. The absorption decreases steadily as the volume ratio is reduced and the system shifts from w/o to o/w emulsions. The lowest absorption intensities are seen for o/w systems at a volume ratio

(47) Heller, D. A.; Barone, P. W.; Swanson, J. P.; Mayrhofer, R. M.; Strano, M. S. *J. Phys. Chem. B* **2004**, *108*, 6905.

Table 1. Dispersion Quality Comparison of Aqueous SWNT Suspensions

	aqueous suspension			
analysis	control	interfacial trapping	ultracentrifugation	two-step interfacial trapping
fluorescence intensity	weak	strong	strong	strong
absorbance features	broad peaks	blue-shifted and resolved peaks	blue-shifted and resolved peaks	blue-shifted and resolved peaks
resonant ratio[a]	0.0118	0.0397	0.0486	0.0406
diameter distribution[b]	12.8 ± 11.9 nm	4.1 ± 3.7 nm		
Raman aggregation ratio[c]	0.7265	1.1868	1.8860	1.5952
F/*A* ratio[d]	0.0135	0.2300	0.5234	0.6077

[a] Calculation based on peak near 660 nm. [b] Distribution determined from AFM and SIMAGIS image analysis. [c] Calculation based on intensity from (11, 3) nanotubes and aggregation peak (~270 cm^{-1}). [d] Calculation based on fluorescence intensity from (7, 6) nanotubes and absorbance at 662 nm.

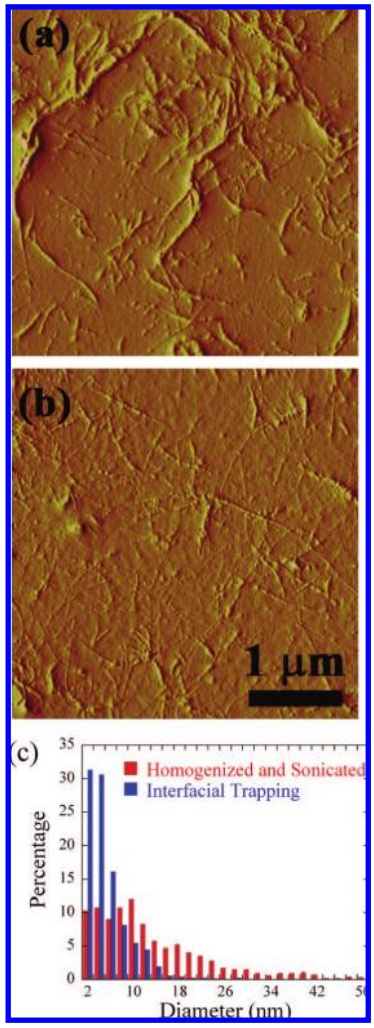

Figure 3. AFM images of gum Arabic SWNT suspensions after (a) homogenization and ultrasonication and (b) after bundle removal by interfacial trapping. (c) Histogram of nanotube diameters measured from the AFM images. The suspension was prepared from an initial concentration of 0.2 mg/mL raw SWNTs.

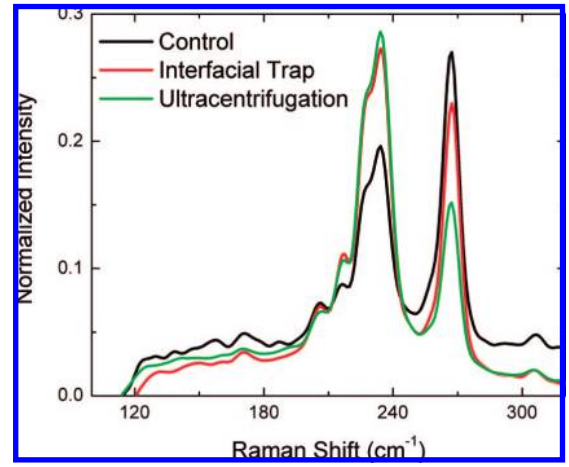

Figure 4. Normalized Raman spectra of the RBMs (ex = 785 nm) for gum Arabic-suspended SWNTs after homogenization and ultrasonication (black line), interfacial trapping (red line), and ultracentrifugation (green line). The suspension was prepared from an initial concentration of 0.2 mg/mL raw SWNTs.

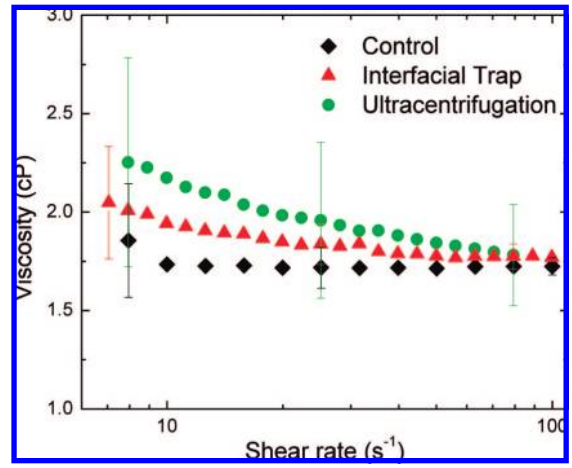

Figure 5. Steady values of the shear viscosities for the gum Arabic-suspended SWNTs produced after homogenization and ultrasonication (control), interfacial trapping, and ultracentrifugation. The suspensions were prepared at similar concentrations to enable comparison. The final concentration of the control, interfacial trapping suspension, and ultracentrifuged samples were 0.02, 0.026, and 0.025 mg/mL, respectively.

of $R = 0.5$. Figure 7b plots the *F*/*A* ratio as a function of the volume ratio. Higher *F*/*A* ratios are seen for o/w systems when compared to w/o systems indicating that a higher fraction of individual nanotubes are suspended in o/w systems via interfacial trapping.

To further improve the quality of the suspensions, a second interfacial trapping step was introduced. The SWNT suspension was first mixed with toluene at a volume ratio of $R = 0.1$ since o/w emulsions were the most effective at removing bundled nanotubes from the aqueous phase. The aqueous phase was separated from the oil and interphase and then mixed again with toluene at a volume ratio of $R = 0.1$. As seen in Figure 8a, the second interfacial trap has little effect on the fluorescence intensity. However, the absorbance spectrum shown in Figure 8b has decreased significantly, resulting in significant changes to the fraction of bundled SWNTs (see Figure S3 in the Supporting Information). The Raman aggregation peak has also shown further improvement after the second interfacial trapping

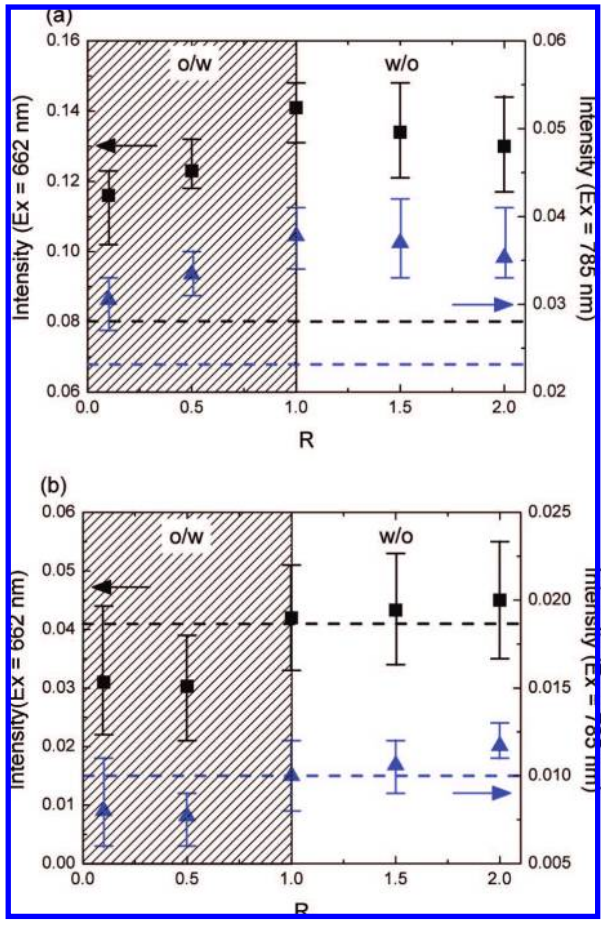

Figure 6. Fluorescence emission intensity fluctuations of the (7, 6) nanotube as a function of the volume ratio (R). The sample was prepared from an initial mass concentration of (a) 0.03 or (b) 0.005 mg/mL raw SWNTs. Excitation is at 662 (■) and 784 nm (▲). Conductivity measurements suggest the formation of oil-in-water (o/w) emulsions (shaded area) for $R < 1$ and water-in-oil emulsions (w/o) for $R > 1$. The dashed lines represent the fluorescence spectra for the suspension after homogenization and ultrasonication.

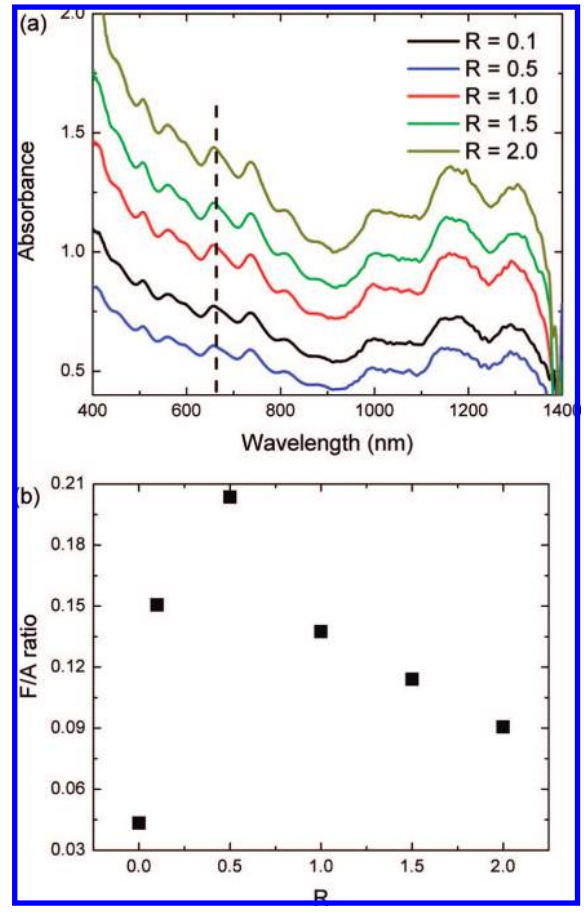

Figure 7. (a) Absorbance spectra of gum Arabic-suspended SWNTs and (b) fluorescence to absorbance ratio fluctuations as a function of the volume ratio (R). The fluorescence intensity was measured for the (7, 6) nanotube and divided by the absorbance at the excitation wavelength (dashed line at 662 nm). The suspension was prepared from an initial concentration of 0.03 mg/mL raw SWNTs.

step as shown in Figure 8c. It is important to note that changes to both Raman and absorbance spectra without changes to the fluorescence provide strong evidence that the interfacial trapping process is highly selective in the removal of bundled SWNTs from the aqueous phase. Table 1 summarizes the dispersion quality measurements for the two-step interfacial process compared to ultracentrifugation. As seen in the table, interfacial trapping shows better dispersion than ultracentrifugation by the *F*/*A* ratio and comparable dispersion quality when characterized by Raman and absorbance spectra.

Interfacial Trapping Mechanism. Figure 9 shows a conceptual diagram of the overall two-phase interfacial trapping process based on experimental observations. First, nanotubes are homogenized and ultrasonicated in a surfactant solution resulting in a suspension that contains both individually dispersed and bundled SWNTs. An immiscible organic solvent is added to the aqueous suspension forming a two-phase system. This two-phase system is then mixed resulting in emulsions (either o/w or w/o depending on the volume ratios) as shown previously.[15] SWNT bundles preferentially adsorb at the emulsion interface when mixed. The emulsions then coalesce into a continuous phase with some emulsions being stabilized by the SWNT bundles. Finally, phase separation into an organic phase, an interphase of stabilized emulsions, and a transparent aqueous phase allows easy collection of the individually suspended SWNTs.

Although bundled nanotubes have been removed from the aqueous phase at all volume ratios (see Figures 6 and 7), the slight decrease in emission intensity for o/w systems indicates that individual SWNTs are removed from the aqueous phase. This conclusion is also confirmed by correcting the absorbance spectra for the nonresonant background (Figure S4 in the Supporting Information). This data suggests that o/w emulsions are more effective in removing nanotubes from the aqueous suspension. The preferential adsorption of hydrophilic silica particles in o/w emulsions was also seen by Binks and co-workers.[48,49] Adjusting the hydrophilicity of the particles had significant effects on the contact angle and their ability to stabilize the emulsions. The individual and bundled nanotubes are coated with hydrophilic surfactants also providing better stabilization of o/w emulsions and, hence, removal from the aqueous phase. In contrast, individual, gum Arabic-coated nanotubes do not seem to stabilize w/o interfaces as effectively which results in nanotube bundles being the primary constituent of the interface. This could indicate that the system contains a small fraction of uncoated (hydrophobic) or poorly coated nanotube bundles that stabilize w/o emulsions.

Selective partitioning of SWNT bundles to the interface can be understood by describing the initial driving force of a single

(48) Binks, B. P.; Lumsdon, S. O. *Langmuir* **2000**, *16*, 8622.
(49) Binks, B. P.; Clint, J. H. *Langmuir* **2002**, *18*, 1270.

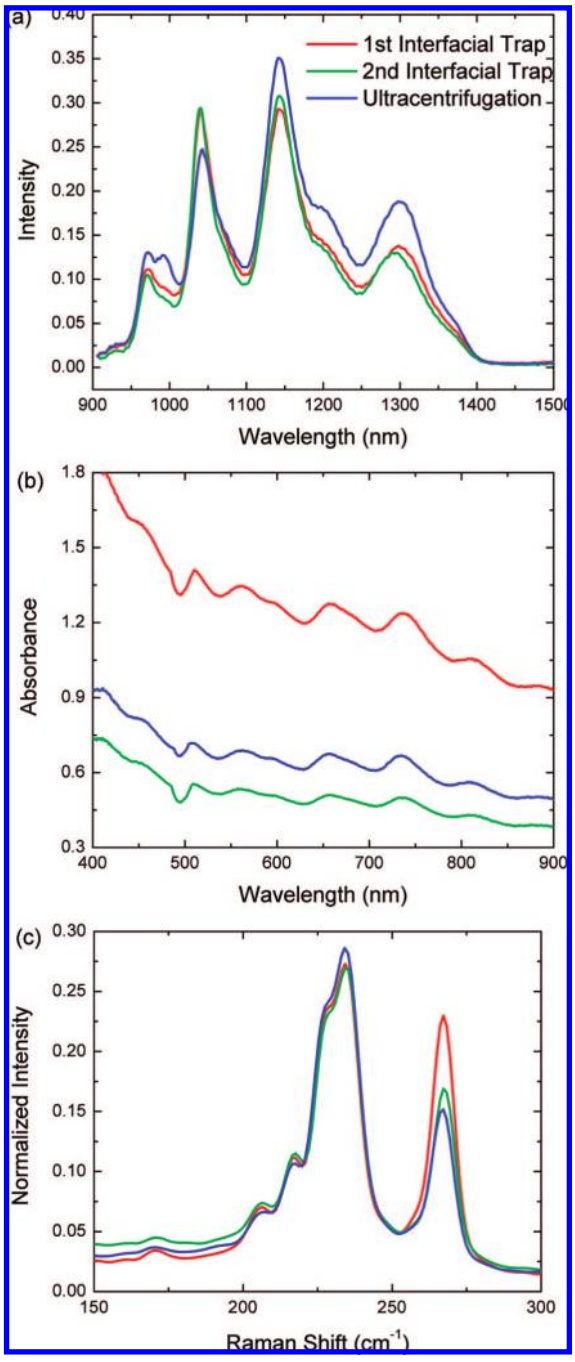

Figure 8. (a) Fluorescence (ex = 662 nm), (b) absorbance, and (c) Raman RBM spectra (ex = 785 nm) of gum Arabic-suspended SWNTs for one-step and two-step interfacial trapping separations compared to ultracentrifugation. The suspensions were prepared from an initial concentration of 0.2 mg/mL raw SWNTs.

nanotube by free energy minimization. These simple models do not account for entropic or kinetic effects but have described interfacial assembly of nanoparticles as small as 2.8 nm.[19,24,48−50] Initially, the nanotubes are dispersed in the aqueous phase as shown in Figure 10a. If both individual and bundled SWNTs are transferred to the oil−water interface upon mixing, the nanotubes will have a contact angle θ measured into the aqueous phase (see Figure 10b). On the basis of experimental evidence[29] and calculations,[20] SWNTs are expected to orient parallel to

(50) Manoharan, V. N. *Solid State Commun.* **2006**, *139*, 557.

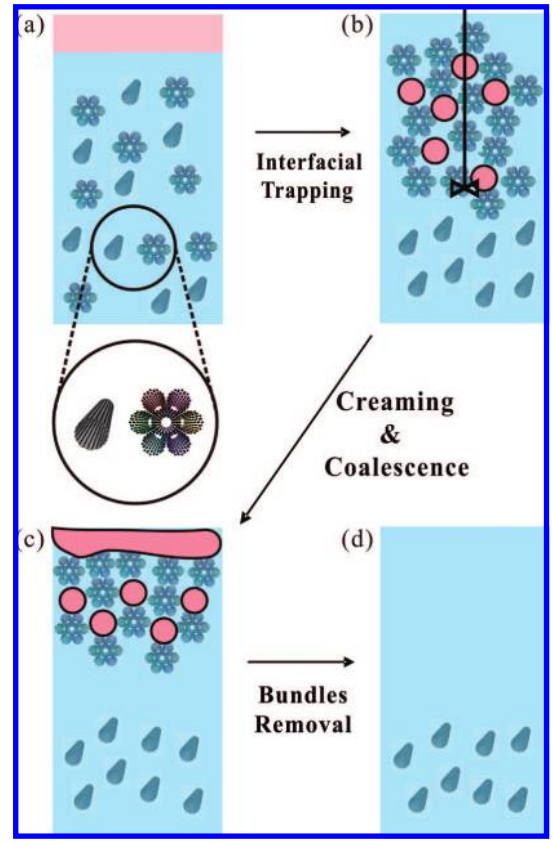

Figure 9. Overall process of removing SWNT bundles from aqueous suspensions via liquid−liquid interfaces. Prior to interfacial trapping, the raw SWNTs are first homogenized with a high-shear mixer and ultrasonicated to coat SWNTs with surfactant (not shown), resulting in a mixture of individually suspended SWNTs and SWNT bundles. (a) Toluene is added to the aqueous phase and mixed to form emulsions, (b) SWNT bundles are trapped at the emulsion interfaces, (c) creaming and coalescence of emulsions separates the bundled SWNTs, and (d) SWNT bundles are removed from the bulk aqueous fluid.

the interface. Therefore, the decrease in interfacial area for inserting a cylindrical particle of radius (R_{SWNT} or R_{bundle}) and length (L) between the oil and water phases is given by the expression, $\Delta A_{ow} = 2RL \sin\theta$, as shown in Figure 10b. The position of the SWNT at the interface depends on the contact angle and results in a loss of particle interactions with the aqueous phase as well as increased interactions with the oil phase. If the interface is assumed planar and the weight of the nanotube is ignored, the energy change upon inserting the nanotube at the interface is

$$\Delta E = 2\pi RL\left(\frac{2\theta}{360^\circ}\right)(\gamma_{po} - \gamma_{pw}) - 2RL\gamma_{ow}\sin\theta \qquad (1)$$

where γ_{po}, γ_{pw}, and γ_{ow} are the interfacial tensions at the particle−oil, particle−water, and oil−water interface, respectively. If ΔE is negative as expected for hydrophilic particles, the particle will be in a stable position at the interface. Substituting Young's equation, $\gamma_{po} - \gamma_{pw} = \gamma_{ow}\cos\theta$, into eq 1, the energy change for inserting a nanotube at the oil−water interface is

$$\Delta E = 2RL\gamma_{ow}\left[\frac{\pi\theta}{180^\circ}\cos\theta - \sin\theta\right] \qquad (2)$$

The contact angle will be similar for individual and bundled nanotubes because of their similar hydrophilicity, and γ_{ow} is fixed in the system. Therefore, in aqueous SWNT suspensions,

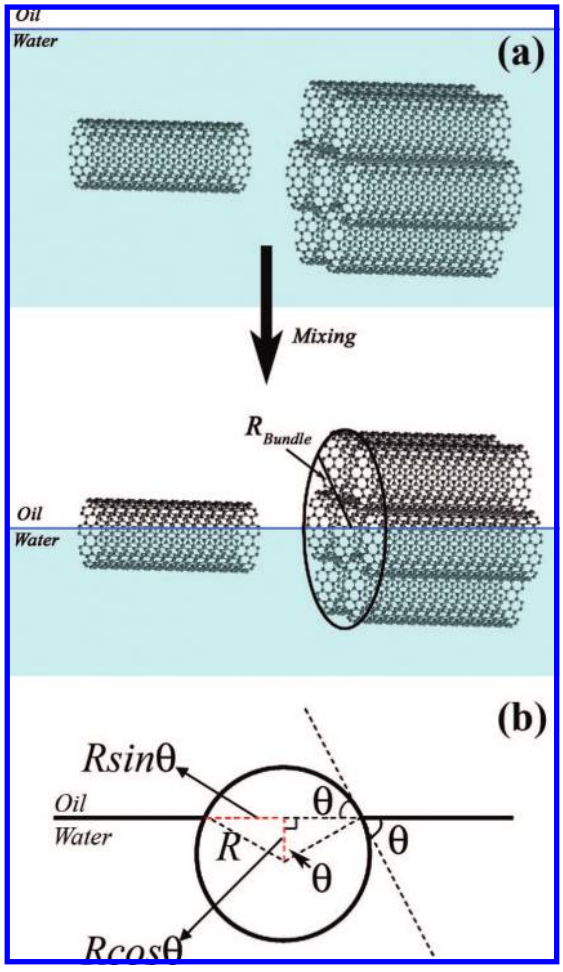

Figure 10. Adsorption process of an individual or bundle of nanotubes at the interface of the oil and water phases. (a) Prior to interfacial trapping, individual or bundled nanotubes are dispersed in the aqueous phase. After mixing, the nanotubes assemble at the interface. (b) Diagram showing the end of a nanotube at the interface where R is the radius of an individual or bundled nanotube and θ is the contact angle measured into the water phase.

the change in energy of inserting a particle at the interface depends on R and L. As seen in eq 2, the energy is minimized when particles with larger radius and length are at the interface. For example, it is estimated that ΔE is approximately $-200kT$ for an individual nanotube and $-4500kT$ for a bundle of the same length containing 7−10 nanotubes. Note from eq 2 that longer SWNTs will be preferentially removed from the suspension. Therefore, these estimates for ΔE are likely the minimum initial driving force since bundles have lengths longer than individual nanotubes. These calculations are in agreement with the experimental results presented above as well as the results of Yi et al.,[31] which showed reduced emulsion stabilization for short-length multiwalled nanotubes. The relatively large negative free energy indicates that both individual and bundled SWNTs prefer to reside at the interface. This explains why o/w emulsions showed decreases in fluorescence intensity in Figure 6b and fewer individual SWNTs in the corrected absorbance (see Figures S3 and S4 in the Supporting Information). On the other hand, there will be a competition for the limited interfacial sites in systems with high initial concentration, where the bundles will be preferred because of the greater driving force.

Conclusion

SWNT bundles can be removed from an aqueous suspension of individual SWNTs by interfacial trapping. This technique offers a simple route to achieve large-scale production of aqueous SWNT suspensions. The significant decrease in absorbance intensity and the Raman aggregation peak combined with increases in fluorescence intensity suggests that nanotube bundles are selectively removed from the aqueous suspension. Although the quality of SWNT dispersions of a single interfacial trapping step is lower than that of the established ultracentrifugation method, different processing conditions and multiple extraction steps improve the dispersion quality, making it comparable to ultracentrifugation. A simple model is developed to describe the changes in free energy and helps explain why SWNT bundles preferentially exist at the interface, yielding effective separations.

Acknowledgment. We acknowledge financial support from the University of Florida. We also thank Dr. Yiider Tseng for access to the ultracentrifuge and the Richard Smalley Institute at Rice University for supplying the nanotubes.

Supporting Information Available: Absorbance and fluorescence intensity as a function of concentration, comparison of corrected absorbance for interfacial trapped and ultracentrifuged suspensions, and corrected absorbance as a function of volume ratio. This material is available free of charge via the Internet at http://pubs.acs.org.

JA804982B